Earthquakes and Structures, *Vol. 7, No. 6 (2014) 1045-1060*
DOI: http://dx.doi.org/10.12989/eas.2014.7.6.1045

Effect of reducing tsunami damage by installing fairing in Kesen-Bridge

Takahiro Abukawa*[1], Yuto Nakamura[2] and Akira Hasegawa[2]

[1]*Department of Design, CHODAI, Sendai 984-0051, Japan*
[2]*Department of Civil Engineering, Hachinohe Institute of Technology, Hachinohe 031-8501, Japan*

(Received March 7, 2014, Revised May 20, 2014, Accepted June 9, 2014)

Abstract. The 2011 off the Pacific coast of Tohoku Earthquake brought serious damage around the Tohoku district in Japan, and much human life and fortune were lost. Bridges were damaged by this earthquake. It was the most serious damage that the superstructures of bridges were flowed out by tsunami. Earthquakes of the same scale are predicted in other areas of Japan. It is necessary to take measures for bridges near coast. In order to understand the tsunami force acting on the bridge, hydraulic model experiments was conducted. In addition, this paper focused on fairing that is effective in wind resistant stability. Installing fairing to bridges has been verified by experiments whether it is possible to reduce the force of tsunami.

Keywords: tsunami; Kesen-Bridge; fairing; hydraulic model experiment, mechanism of tsunami action for bridge

1. Introduction

The 2011 off the Pacific coast of Tohoku Earthquake brought serious damage around the Tohoku district in Japan, and much human life and fortune were lost. Although many bridges suffered damage from this earthquake, the damage in which superstructure was flowed out by tsunami was the most serious.

Especially, as for Kesen-Bridge which was erected on National Highway, superstructure was flowed out to about 300m upper stream. Therefore, National Highway which is an important route was blocked off, and it became a significant delay in relief and restoration. Important highways are required to ensure the function, as an emergency route in disaster. It is necessary to carry out tsunami resistant design along with earthquake resistant design. However, tsunami resistant design has not yet been established. Large earthquakes have been predicted in Japan, measures are needed.

Tsunami off the west coast of northern Sumatra earthquake 2004 since occurrence, researches have been advanced about influence on bridge by tsunami. Kosa *et al.* (2007) conducted a damage survey of the bridge by the tsunami of Sumatra earthquake. Furthermore, it is verified by the numerical analysis for bridge damaged. According to the research of Nii *et al.* (2009), experiments have been conducted to evaluate the tsunami force acting on the RC simple girder bridge.

*Corresponding author, Engineer, E-mail: abukawa-t@chodai.co.jp

Copyright © 2014 Techno-Press, Ltd.
http://www.techno-press.org/?journal=eas&subpage=7 ISSN: 2092-7614 (Print), 2092-7622 (Online)

According to research on Zhang *et al.* (2010), they conducted experiments installed fairing on the side of the RC simple girder bridge that was damaged by the Indian Ocean Tsunami. In the experiment, effectiveness of the fairing is shown.

In this paper, in order to elucidate the tsunami force acting on the bridge, the authors conducted hydraulic model experiments in Kesen-Bridge which was a steel girder bridge. In addition, the authors were verified effect of the fairing which was installed on bridge, and focused on the effectiveness of two kinds of fairing shapes. One is fairing of Box-shape to be installed so as to surround the bridge girder. Another is fairing of L-shape to be installed on side of bridge girder. This paper verified whether it is possible to reduce force of tsunami, by installing these fairings.

2. Damage situation in the earthquake

Feature of this earthquake is that the epicenter was Sanriku offshore in Pacific Ocean. Therefore, the damage caused by the tsunami was outstanding than the damage caused by the seismic motion. Ministry of Land, Infrastructure and Transport Tohoku Regional Development Bureau in Japan investigated the 1572 bridges after the earthquake. Bridges affected by the tsunami were 151 bridges and about 10% of the 1572 bridges. However, the damage ratio in the disaster caused by the tsunami was found to be as high as 93.4% shown in Fig. 1.

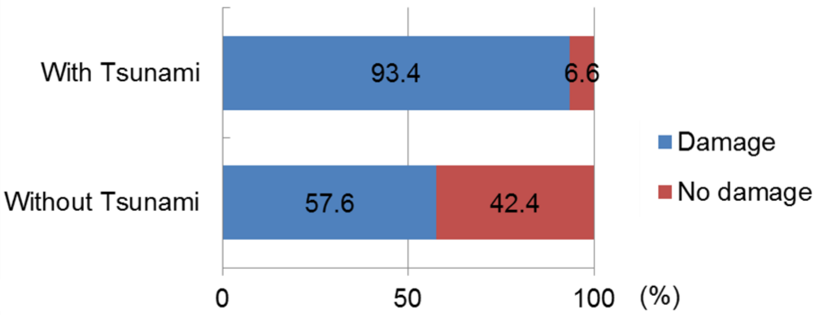

Fig. 1 Influence and damage of tsunami

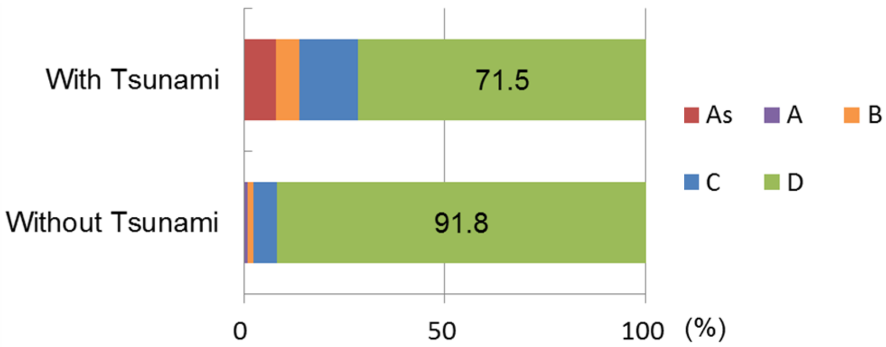

Fig. 2 Damage on load-bearing capacity of bridges by the tsunami

Fig. 2 shows the damage on the load-bearing capacity of bridges by the effect of the tsunami. Disaster degrees are rated from As to D.

As : collapse of bridge.
A : great damage (fatal damage and significant decrease in load bearing capacity)
B : middle damage (vehicle passable and slight decrease in load bearing capacity.)
C : small damage (slight damage)
D : no damage

Fig. 2 shows that the collapse of bridges can be seen only in bridges affected by the tsunami. The degree of damage in the bridges becomes higher in bridges affected by the tsunami. Therefore, the damage of the bridge has been found to increase by the tsunami action. In the specifications of Japan for highway bridges revised after the earthquake, the structure plan for disaster prevention must consider tsunami impact for the structures located near seashore. In the specification, as examples for measures to prevent the damage by tsunami, less affective structure of tsunami and structures that are easy to recovery even if the bridges were damaged are introduced.

3. Overview of the experiment

3.1 Kesen-Bridge (Bridge model)

Kesen-Bridge had been built on national highway 45 in Iwate prefecture. Bridge type is a steel continuous girder bridge, the length is 181.5m, and span length is 35.97m. It is constituted by the 3 span and 2 spans. Superstructure is completely flown out to about 300m upstream by the tsunami,

Fig. 3 Damaged Kesen-Bridge

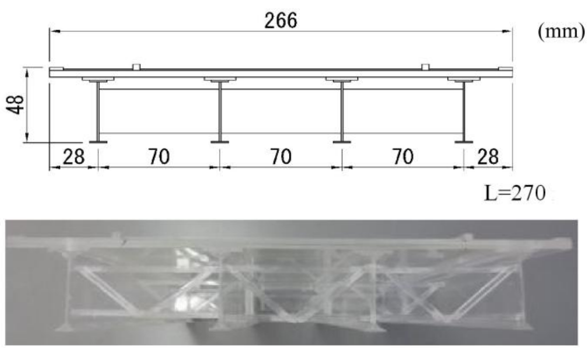

Fig. 4 Sectional view of the Kesen-Bridge model

and pavement surface had been peeled off by the erosion of the embankment. Temporary bridge is now serviced. Fig. 3 shows disaster situation of Kesen-Bridge, and Fig. 4 shows a sectional view of the Kesen-Bridge model. Considering the size of experimental flume, bridge model was set at scale 1/50.

3.2 Experimental flume

Fig. 5 shows photos of experimental flume, sluice gate, and side of sluice gate. Fig. 6 shows side view of experimental flume and cross-sectional view. Total length of the experimental flume is 16.99m; upstream side and downstream side are 5.69m, 11.30m in length respectively. Sluice gate of stainless steel is disposed between them.

Waves are generated by pulling up the sluice gate. Experiments were carried out by installing the bridge model to position of 5.0m from sluice gate. Partition plate was installed to split the flume. Bridge model was installed on the right side; current meter was installed on the left side.

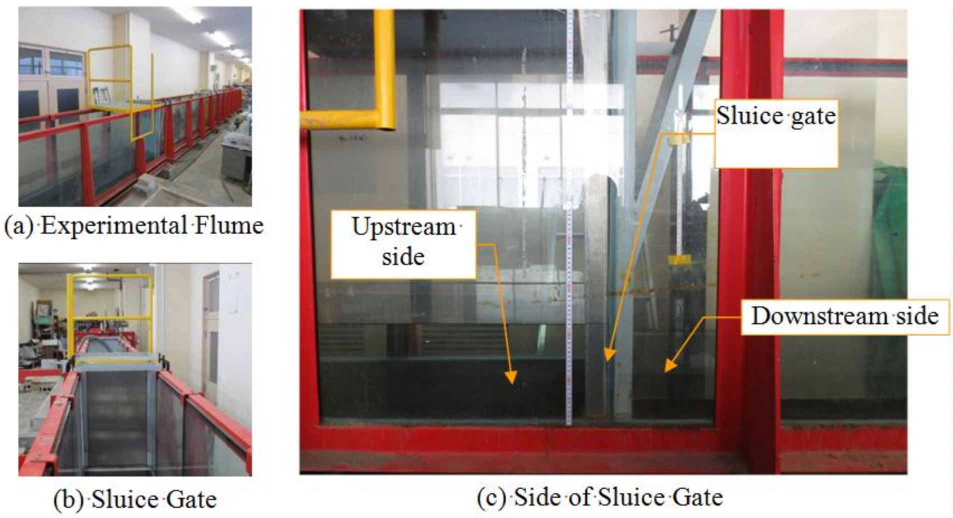

Fig. 5 Experimental situation

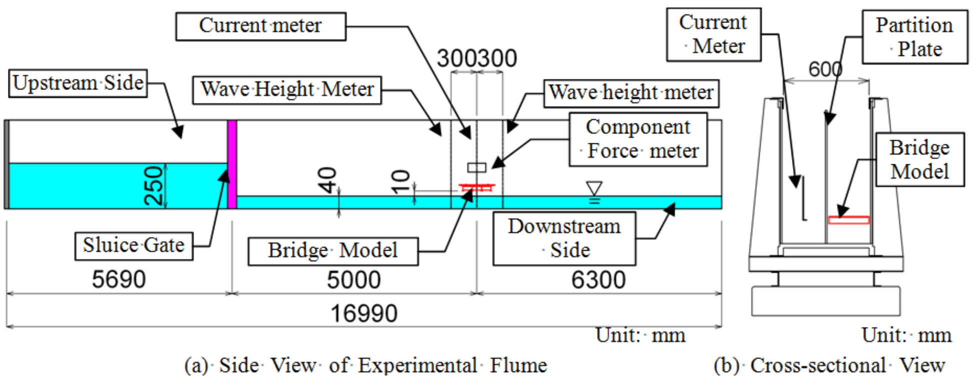

Fig. 6 Experimental flume

3.3 Measurement equipment

Fig. 7, and 8 show installation status of the measuring equipment. Measurement equipment is the following configuration; component force meter (horizontal and vertical), wave height meters, current meter. Component force meter was installed in the top of bridge model. Wave height meter was installed at position upstream and downstream 30cm from center of the bridge model. Current meter was installed on back side of the partition plate; on center position of the bridge model. In addition, situations of the wave collision were taken with a video camera from the side.

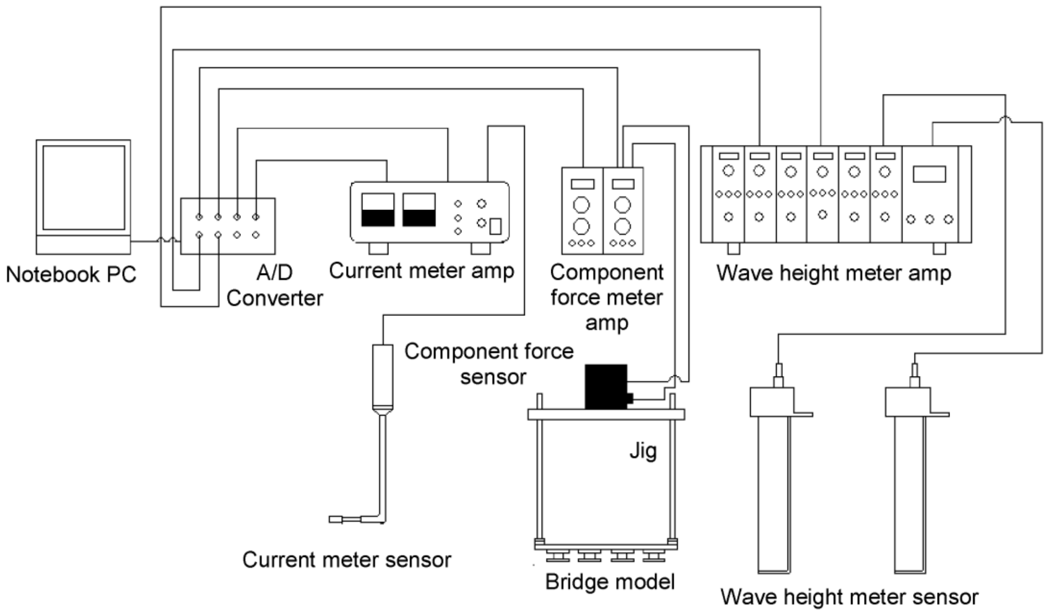

Fig. 7 Measuring equipment

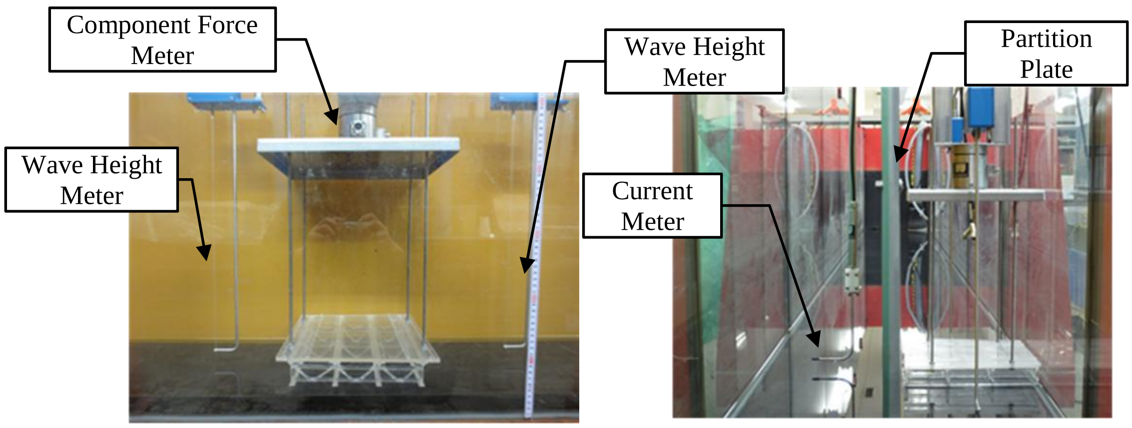

(a) Side (b) Front

Fig. 8 Installation conditions

3.4 Flow velocity

It is estimated the average of flow velocity of the tsunami is 7.0m/sec (Zheng 2013), from video of suspended matter to be swept away by the tsunami in the vicinity of Kesen-Bridge. Therefore, the flow velocity of the experimental wave was calculated as constant Froude number.

The scale 1/50 was used considering experimental conditions experimental flow velocity V_M was set to be 1.0m/sec from Eq. (1), (2) and (3). Therefore, calibration was performed. As a result, by setting water level upstream and downstream for 25cm and 4cm, the experiment flow velocity was found to be 1.0m/sec. However, the flow velocity had not accord exactly with 1.0 m/sec. Considering horizontal drag is derived from Eq. (4), measured value is corrected by Eq. (5). In this paper, the experimental value indicates a value after correction.

$$Fr = \frac{V_R}{\sqrt{gL_R}} = \frac{V_M}{\sqrt{gL_M}} \tag{1}$$

$$N = \frac{L_R}{L_M} \tag{2}$$

$$V_M = V_R\sqrt{\frac{L_M}{L_R}} = \frac{V_R}{\sqrt{N}} = \frac{7.0}{\sqrt{50}} = 1.0m/\sec \tag{3}$$

$$F = \frac{1}{2}\rho_w \times C_d \times A \times V^2 \tag{4}$$

$$F_M = F_{Mi} \times \frac{{V_M}^2}{{V_{Mi}}^2} = F_{Mi} \times \frac{1.0}{{V_{Mi}}^2} \tag{5}$$

where is V_R: is flow velocity of the real (2011 tsunami), V_M is flow velocity of the model, L_R is length of the real, L_M is length of the model, g is acceleration of gravity, N is scale, ρ_w is water density, C_d is drag coefficient, A is projected area, V is flow velocity.

4. Mechanism of tsunami action

Fig. 9 shows a situation in which tsunami was acting to Kesen-Bridge model after reaching at the side of the model. The upper figure in Fig. 9 shows the time history curve of the horizontal force and vertical force acting on the bridge model. The lower pictures in Fig. 9 show the shapes of tsunami wave in different time. The positive direction of horizontal force and vertical force are right and downward, respectively.

(a) Tsunami begins to act on the bridge model

The horizontal force started to the action to the model, on the other hand, the vertical force showed no big change. Tsunami wave acted only to the bottom of the main girder.

(b) Impact force has the maximum value

The horizontal force has the maximum value. The vertical force is the minimum, conversely. Tsunami acts on the all left aspect of the bridge model. A part of tsunami wave is reflected back by hitting the girder. A part of tsunami wave has jumped over the bridge model. In the lower part of the model, the installing of water has begun.

(c) Immediately after the impact force is acted

The reflection of a part of wave is seen. However, majority of tsunami wave is jumped on the model. Because the tsunami wave is applied to the entire bottom of the main girder, the vertical force is exerted upward on the bridge model whole.

(d) Vertical force is maximum value

The majority of jumped tsunami wave dropped down to the surface of the bridge model. Tsunami wave of the left aspect end is changing gently. Whole of bridge model is in the turbulent flow, horizontal force is changing to steady force from impact force.

(e) and (f) Movement of a steady wave

Tsunami waves acting on the bridge model have changed gently. Air is trapped in the interior of the girder. In this period, vertical force and horizontal force show similar values. Force pressing the bridge from the top is exerted long period of time.

Impact force is maximized when the wave hits the bridge model. Steady force became about 1/3 of the maximum value. Vertical force has the strong force upward when the wave hits the bridge model. On the other hand, vertical force has strong force downward when steady force acts. From the pictures in Fig. 9, tsunami wave into the bottom of the bridge model generates the floating force, and then tsunami waves jumped to bridge model will push down the bridge model in long time.

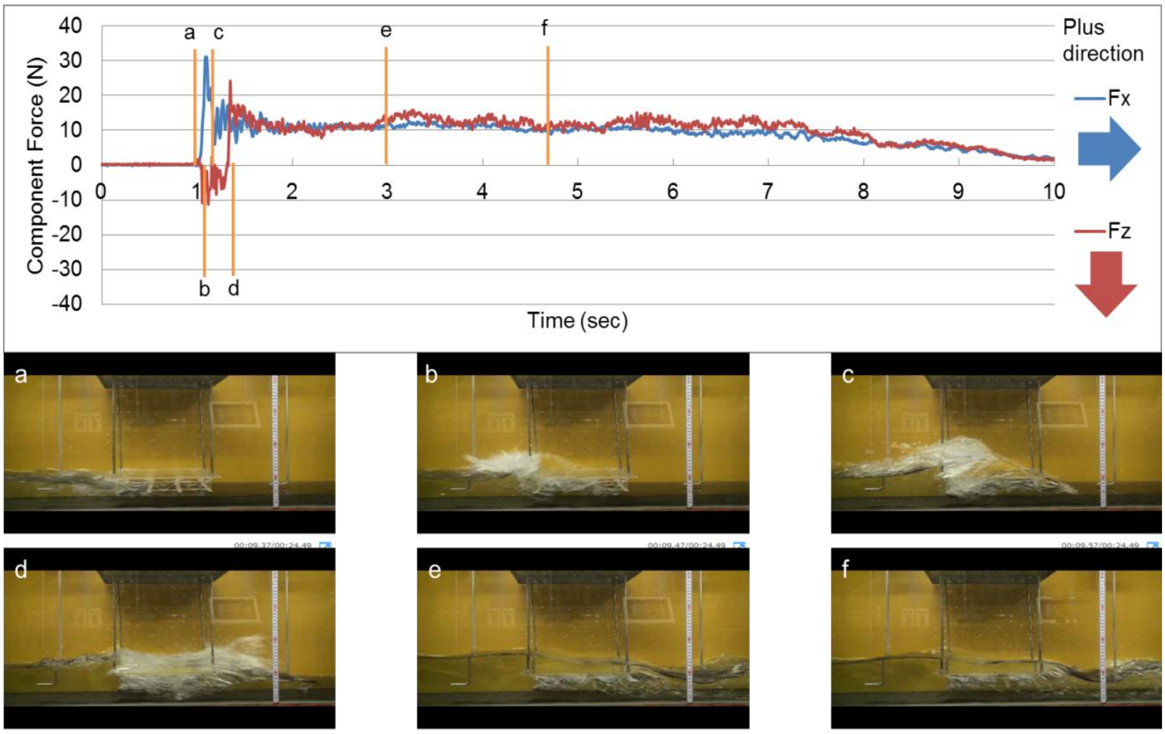

Fig. 9 Time history curve of the component forces and shapes of tsunami wave

5. Experiment of the fairing

5.1 Shape of the fairing

Two shapes for fairings were prepared. Those are Box-shape fairings and L-shape fairings installed in the side surface. L-shapes were set to five types of F1- F5 shown in Table 1. Box-shapes were set to three types of FB0-FB2 shown in Table 2. Side shape of Box-shape fairing was adopted F2 which it had reduced the most force according to the past thesis. The Model that has not installed the fairing is called as F0. Fairing is made of stainless steel and the thickness is 1mm. It has been installed in the model with bolts.

Table 1 L-shape Fairing

	Size(mm)	Cubic diagram
F1	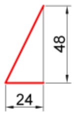	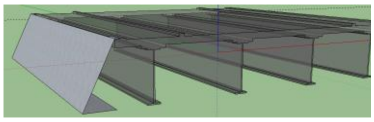
F2	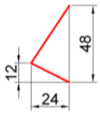	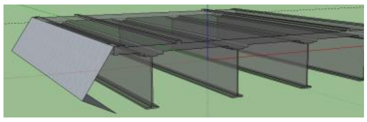
F3	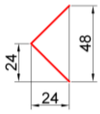	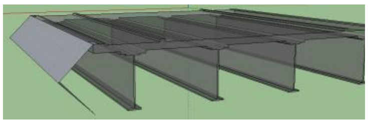
F4	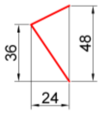	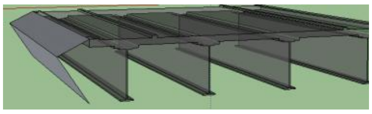
F5		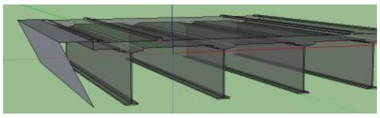

Table 2 Box-shape Fairing

	Size(mm)	Cubic diagram
FB0		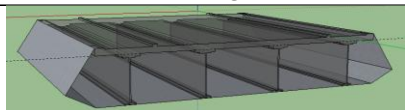
FB1	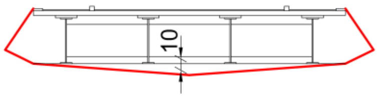	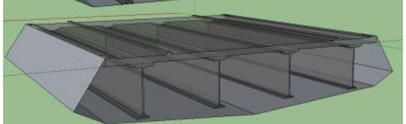
FB2	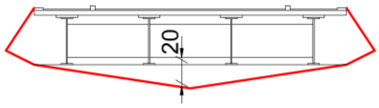	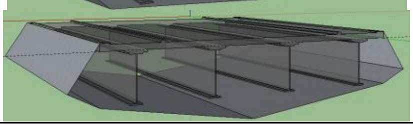

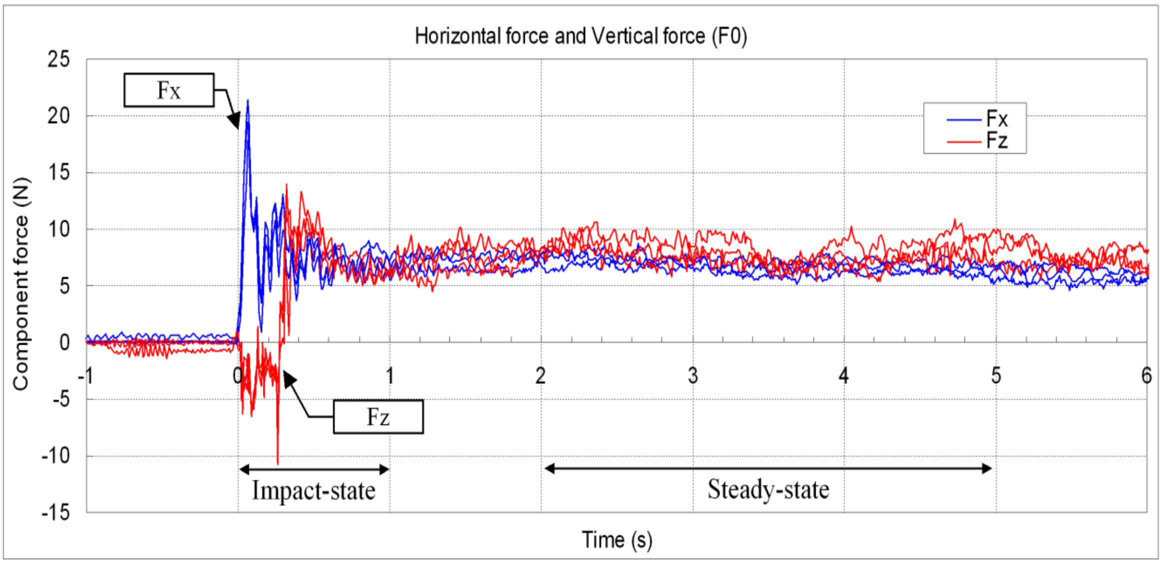

Fig. 10 Time-history waveforms of the force component meter (F0)

5.2 Results and discussions

5.2.1 Situation of waves acting on F0 model (impact-state, steady-state)

In case of F0 which is not installed the fairing, the response waveform of the force component meter is shown in Fig. 10. Value is corrected to the flow velocity 1.0m/sec.

Fx shows horizontal drag. Fz shows force in the vertical direction, in addition positive direction indicates downward force, and negative direction indicates upward force. Fx shows the maximum value immediately after the wave collides. Fz shows the maximum value of upward 0.1 and 0.2 seconds later, after the wave collision. Thereafter, downward force is maximized. Situation which has received the impact force continued about one second. Between 0 and 1.0 seconds after the collision wave are defined as an impact-state. Thereafter, Fz and Fx have remained stable. Between 2.0 and 5.0 seconds after the collision wave are defined as a steady-state. Experiment was carried out three times and the average was calculated.

5.2.2 Effect of L-shape fairing

Table 3 and Fig. 11-13 show the value of the force component meter, at F0 and F1-F5 which were installed L-shape fairing. Fig. 14 shows their waveforms. By installing the L-shape fairing, horizontal drag Fx at impact-state was reduced about 60-90% compared with F0. In particular, F1-F4 were significantly reduced about 60-70% compared with F0. It is considered that the water flow becomes smooth by installing the fairing to the side of the model. Fz (+) was reduced about 70% compared with F0 on steady-state in case of F3, F4. However, upward force is increased in Fz (+) at the impact-state, it cannot be expected the reduction effect for Fz (+). Compared with Fx, Fz can be seen that dispersion is large. Because air is inside the fairing, the air acted as buoyancy without being discharged. Further, it is presumed that discharge of the air is not constant.

Table 3 Maximum Value of The Force Component Meter in L-shape Fairing

			1st	2nd	3rd	Ave	Rate to F0
F0	impact-state	Fx(+)	19.51	17.91	21.39	19.60	—
		Fz(-)	-6.33	-6.56	-10.79	-7.89	—
		Fz(+)	11.52	14.01	13.31	12.95	—
	steady-state	Fx(+)	7.29	6.24	6.84	6.79	—
		Fz(+)	8.81	7.17	7.74	7.91	—
F1	impact-state	Fx(+)	10.94	14.48	9.85	11.76	0.60
		Fz(-)	-13.42	-11.03	-5.60	-10.02	1.27
		Fz(+)	13.63	18.75	12.68	15.02	1.16
	steady-state	Fx(+)	5.15	7.45	5.23	5.94	0.88
		Fz(+)	10.36	13.90	9.82	11.36	1.44
F2	impact-state	Fx(+)	13.13	14.91	13.83	13.96	0.71
		Fz(-)	-8.29	-8.46	-11.27	-9.34	1.18
		Fz(+)	12.45	15.52	14.50	14.15	1.09
	steady-state	Fx(+)	6.72	7.05	6.52	6.76	1.00
		Fz(+)	11.02	11.60	10.47	11.03	1.40
F3	impact-state	Fx(+)	13.22	12.81	13.04	13.02	0.66
		Fz(-)	-10.78	-20.14	-13.41	-14.77	1.87
		Fz(+)	10.91	13.38	12.61	12.30	0.95
	steady-state	Fx(+)	8.00	8.57	7.45	8.01	1.18
		Fz(+)	5.67	6.05	5.81	5.84	0.74
F4	impact-state	Fx(+)	13.06	14.17	12.19	13.14	0.67
		Fz(-)	-10.62	-8.92	-12.88	-10.81	1.37
		Fz(+)	12.51	13.13	12.78	12.81	0.99
	steady-state	Fx(+)	7.47	8.64	7.98	8.03	1.18
		Fz(+)	4.57	6.19	5.99	5.58	0.71
F5	impact-state	Fx(+)	15.50	16.73	20.02	17.42	0.89
		Fz(-)	-10.82	-11.18	-14.40	-12.13	1.54
		Fz(+)	18.19	15.86	21.22	18.42	1.42
	steady-state	Fx(+)	7.79	7.06	8.07	7.64	1.13
		Fz(+)	11.43	9.08	10.84	10.45	1.32

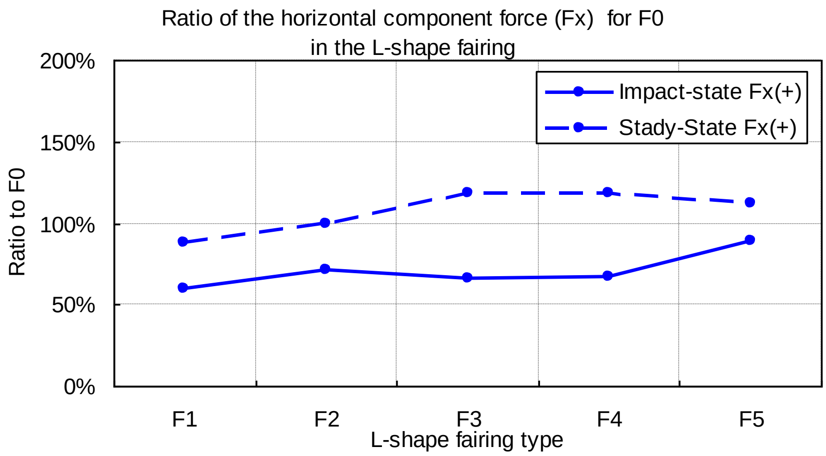

Fig. 11 Ratio of the horizontal component Force (Fx) for F0 in the L-shape fairing

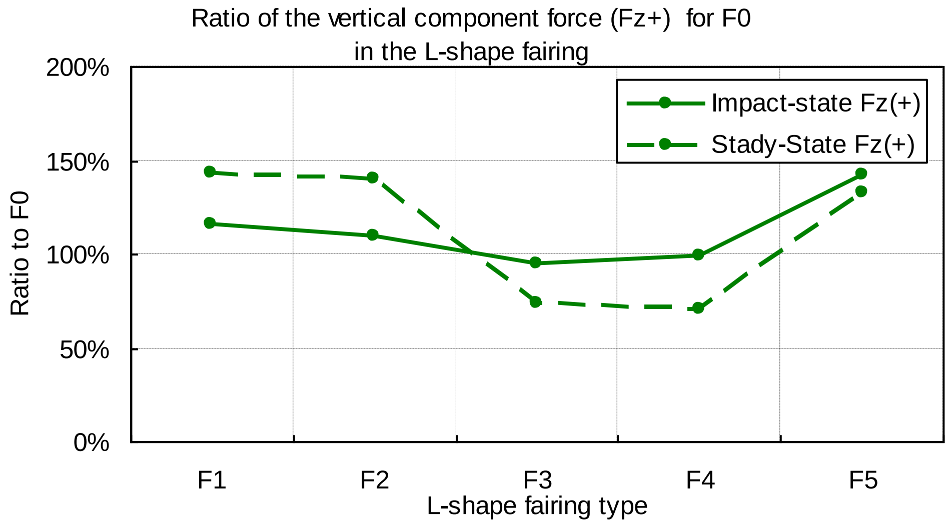

Fig. 12 Ratio of the Vertical Component Force (Fz+) for F0 in the L-shape Fairing

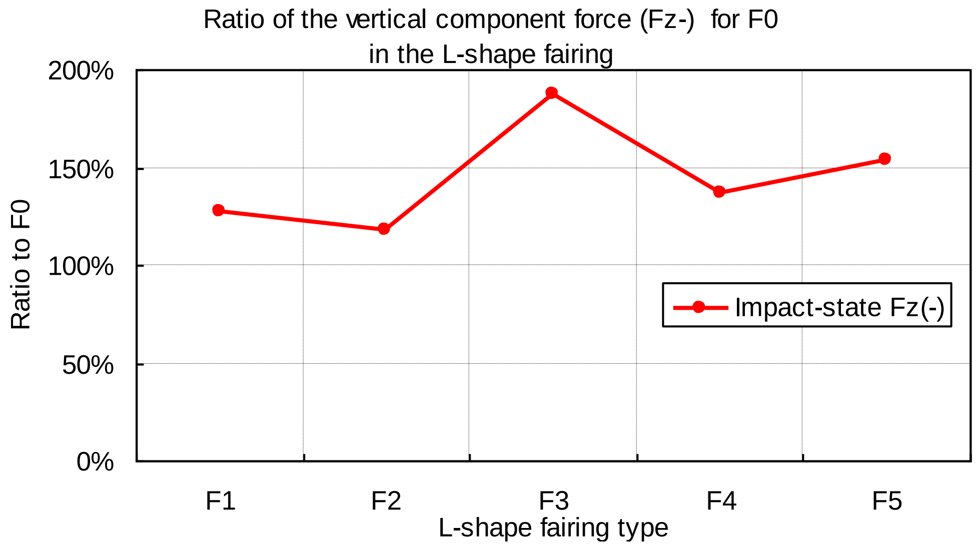

Fig. 13 Ratio of the Vertical Component Force (Fz-) for F0 in the L-shape Fairing

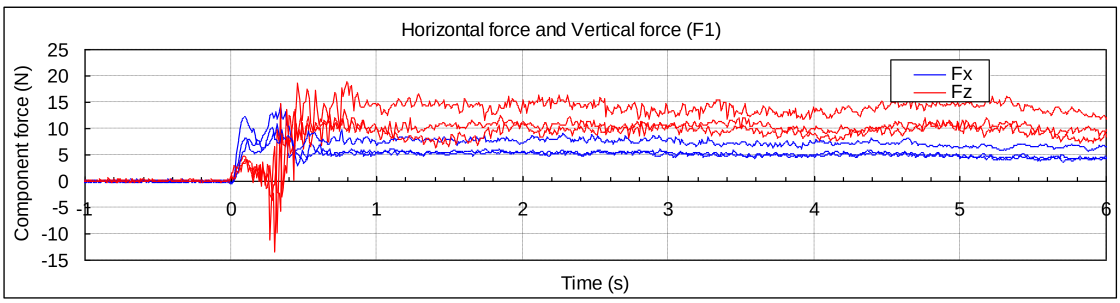

Fig. 14 Time-history Waveforms of the Force Component Meter (F1-F5)

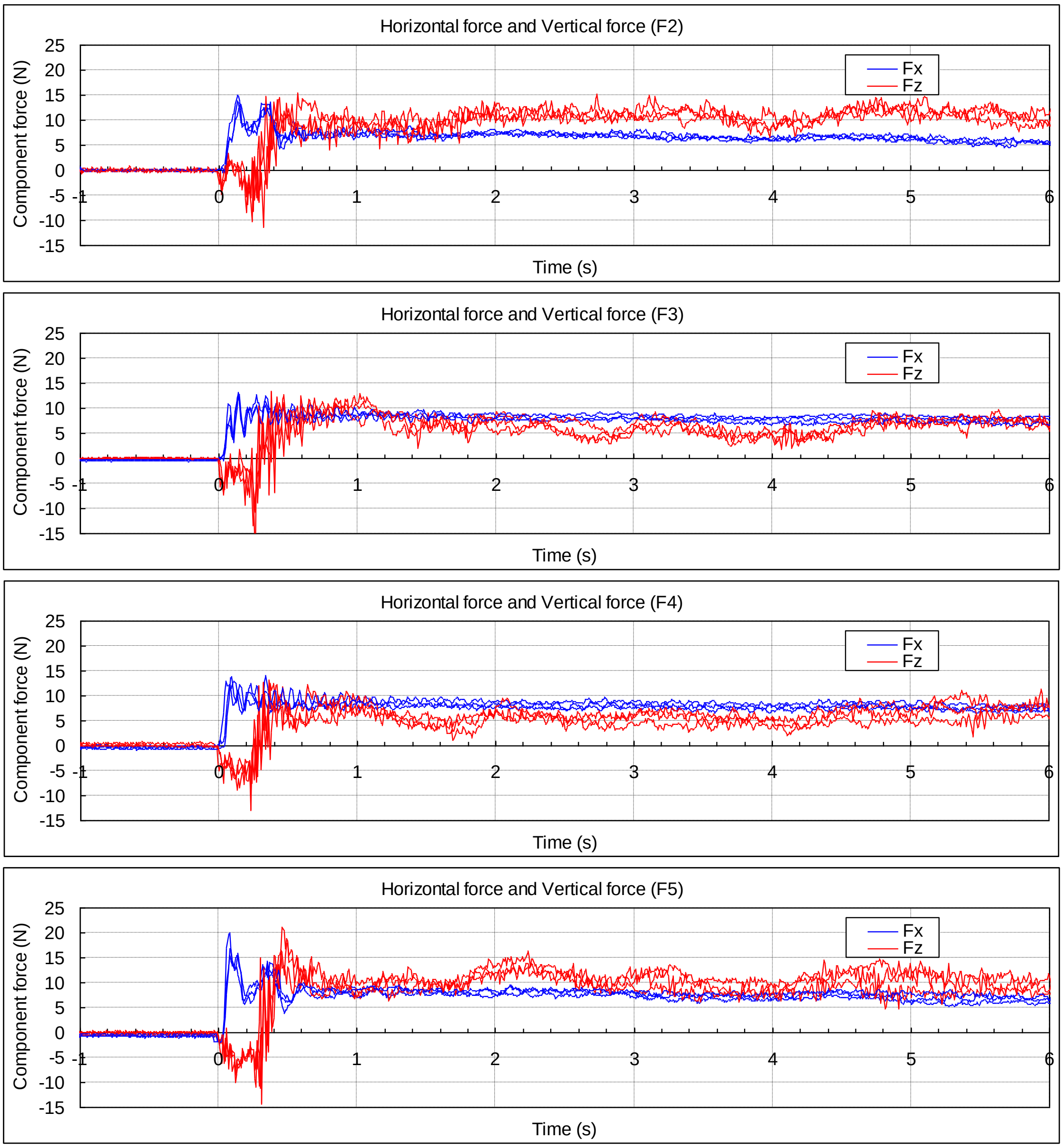

Fig. 14 Continued

5.2.3 Effect of box-shape fairing

Table 4 and Fig. 15-17 show the value of force component meter at FB0-FB2 which were installed Box-shape fairing. Fig.18 shows their waveforms. By installing the

Box-shape faring, horizontal drag Fx at impact-state was reduced about 40-50% compared with F0. In addition horizontal drag Fx at steady-state was reduced about 60-70% compared with F0.

By using Box-shape fairing, better reduction effect of the horizontal drag as compared with the L-shape fairing was obtained. The Box-shape fairing can reduce horizontal resistance value, and so it is possible to smooth the flow of water.

In the vertical force Fz, component forces in both steady-state and impact-state have increased significantly compared with F0. The closed space of the Box-shape receives buoyancy. Table 5 shows buoyancy of the Box-shape fairing. The buoyancy acts as a large upward force, between 36N and 43N. In addition, an upward force is increased in the order of FB0, FB1 and FB2. It seems that upward force was increased because clearance was narrowed, by the fairing was inflated to underside of the main girders.

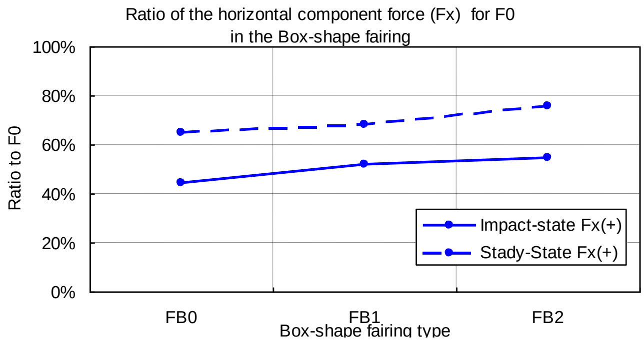

Fig. 15 Ratio of the horizontal component Force (Fx) for F0 in the Box-shape Fairing

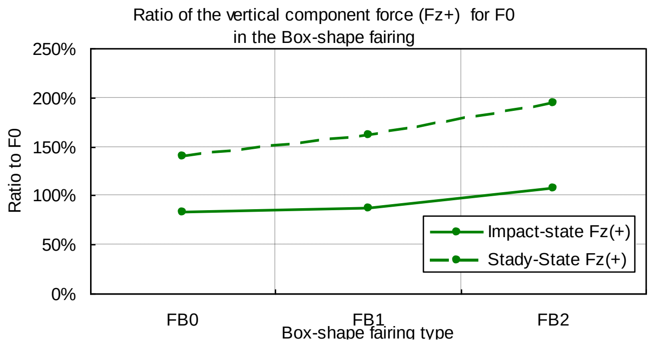

Fig. 16 Ratio of the Horizontal Component Force (Fx) for F0 in the Box -shape Fairing

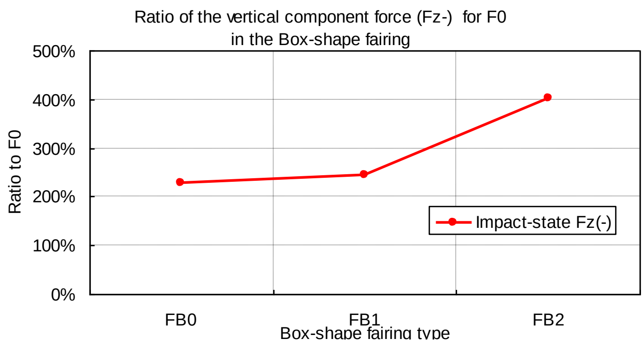

Fig. 17 Ratio of the Horizontal Component Force (Fx) for F0 in the Box -shape Fairing

Table 4 Maximum Value of the Force Component Meter in Box-shape Fairing

			1st	2nd	3rd	Ave	Rate to F0
FB0	impact-state	Fx(+)	8.42	9.36	8.40	8.73	0.45
		Fz(-)	-17.59	-19.07	-17.52	-18.06	2.29
		Fz(+)	9.97	11.62	10.55	10.71	0.83
	steady-state	Fx(+)	4.53	4.44	4.22	4.39	0.65
		Fz(+)	11.65	10.78	10.65	11.03	1.39
FB1	impact-state	Fx(+)	9.14	11.39	9.91	10.15	0.52
		Fz(-)	-18.10	-19.73	-19.96	-19.26	2.44
		Fz(+)	11.40	12.76	9.79	11.32	0.87
	steady-state	Fx(+)	4.49	5.05	4.31	4.62	0.68
		Fz(+)	12.89	13.39	11.91	12.73	1.61
FB2	impact-state	Fx(+)	10.64	10.33	11.17	10.72	0.55
		Fz(-)	-33.36	-26.50	-35.53	-31.80	4.03
		Fz(+)	15.03	12.77	14.11	13.97	1.08
	steady-state	Fx(+)	5.41	5.09	4.93	5.14	0.76
		Fz(+)	16.14	15.55	14.49	15.39	1.95

Table 5 Buoyancy and area of cross section at the box-shape fairing

		FB0	FB1	FB2
area of cross section	m^2	8.42	9.36	8.40
buoyancy	N	36.3	39.8	43.3

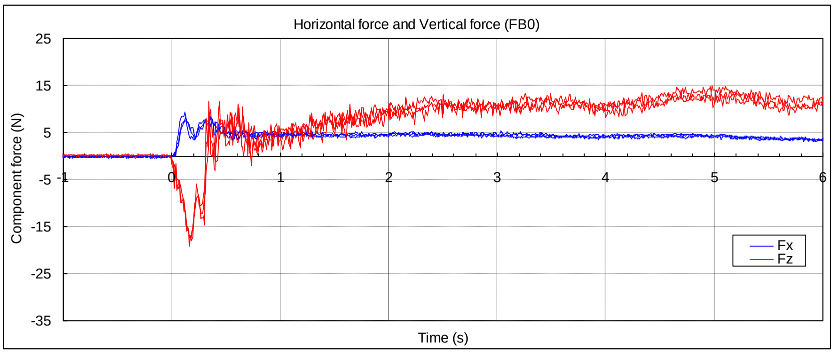

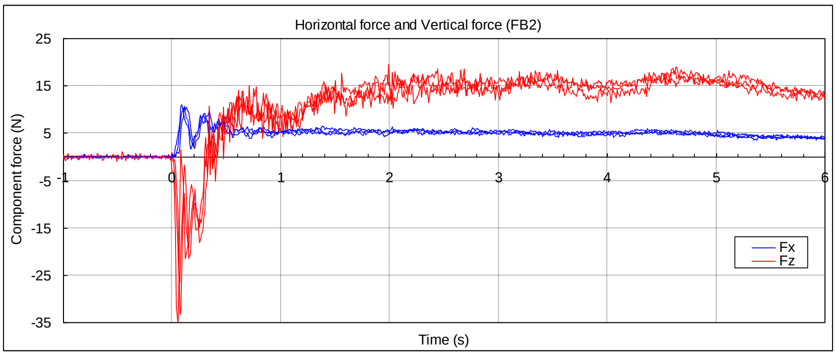

Fig. 18 Time-history Waveforms of the Force Component Meter (FB0-FB2)

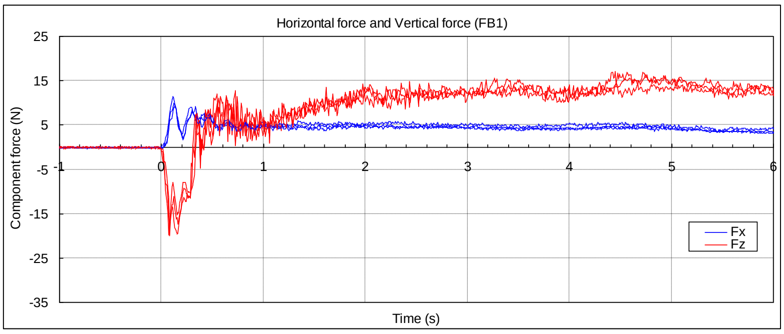

Fig. 18 Continued

6. Conclusion

The experiments were carried out using a model of 1/50 scale of Kesen-Bridge which was damaged by the tsunami in the 2011 off the Pacific coast of Tohoku Earthquake. Purpose of experiments is to verify the effect on the force acting to the bridge by installing Box-shape and L-shape fairing. By considerations on results of experiments, the following conclusions were obtained;

1) By installing the L-shape fairing, it was possible to reduce 60-90% horizontal component force (Fx) at impact-state, as compared with the case of not installed. And in the steady-state, it was possible to reduce about 70% for vertical component force (Fz) in F3 and F4, by installing L-shape fairing. Therefore, it was found that it is possible to reduce component force of both horizontal and vertical, in F4 and F3.

2) Box-shape fairing was possible to significantly reduce the horizontal component force. However, the vertical component force is increased greatly due to the influence of buoyancy. Therefore, it is necessary to solve the problem of buoyancy.

Future task is to examine the fairing shape that can be reduced buoyancy. In addition, experiments on the influence of the fairing angle are planned for reference data to design.

Acknowledgments

We would like to express our appreciation to Tohoku Regional Bureau Ministry of Land , Infrastructure and Transport which provided us with the information on Kesen-Bridge, and Tohoku Construction Association (now, Tohoku Regional Development Association) which provided us with the financial support, and Hachinohe Institute of Technology graduates who supported the experiments.

References

Kosa, K., Uchida, S., Unjho, S. and Shoji, G. (2007), "Investigation and analysis of the damaged bridges due to the sumatora", *J. Earthq. Eng.*, **29**, 895-901.

Itonaga, W., Nakao, H., Izuno, K. and Kobayashi, H. (2012), ”Experimental study on Tsunami forces against plate girder bridge”, *J. JSCE(A1)*, **68**(4), I_1126-I_1133.

Nakao, H., Izuno, K. and Kobayashi, H. (2010), “Study on relation of velocity and wave height to hydrodynamic force on bridges by tsunami”, *J. Struct. Eng.*, **56**(A), 564-575.

Nakao, H., Itonaga, W., Nozaka, K., Izuno, K. and Kobayashi, H. (2012), ”Pressure characteristics of rectangular section girder bridge due to Tsunami”, *J. JSCE(A1)*, **68**(4), I_1145-I_1150.

Nii, S., Kosa, K.,Shoji, G. and Kimura, K. (2009), “Experimental examination concerning tidal wave action power to bridge”, *J. Struct. Eng.*, **55(**1A), 471-482.

Shoji, G., Hiraki, Y., Ezura, Y., Iidaka, M., Fujima, K. and Shigihara, Y. (2012), ”Experimental study on the mechanism of horizontal and vertical wave forces acting on a bridge deck subjected to breaker bores”, *J. JSCE(A1)*, **68**(4) , I_1134-I_1144

Zhang, G., Usui, T. and Hoshikuma, J.I. (2010), “Experimental study on a countermeasure for reducing tsunami wave force acting on superstructure of bridges”, *J. Struct. Eng.*, **66**(1), 425-433.

Zheng, Y. Kosa, K. Fu, L. (2013), “Evaluation for outflow of girder due to tsunami”, *JSCE Annual. Meeting*, **I-029**, 57-58.

IT